Polymer Chemistry

PAPER

View Article Online
View Journal | View Issue

Cite this: *Polym. Chem.*, 2019, **10**, 5200

Aromatic polymers made by reductive polydehalogenation of oligocyclic monomers as conjugated polymers of intrinsic microporosity (C-PIMs)†

Patrick Klein, [a] Hauke J. Jötten,[a] Catherine M. Aitchison, [b] Rob Clowes,[b] Eduard Preis,[a] Andrew I. Cooper, [b] Reiner Sebastian Sprick [b] and Ullrich Scherf *[a]

Received 14th June 2019,
Accepted 6th September 2019

DOI: 10.1039/c9py00869a

rsc.li/polymers

Reductive dehalogenation polycondensation of a series of penta- or hexacyclic, bisgeminal tetrachlorides with dicobalt octacarbonyl leads to the formation of homopolymers and copolymers with very different optical spectra. While the formation of tetrabenzoheptafulvalene connectors introduces efficient conjugation barriers due to their strongly folded structure, linking of 5-membered ring-based pentacyclic building blocks *via* bifluorenylidene connectors allows for an extended π-conjugation along the main chain. A comparison of homopolymer **P57** and copolymer **P55/77** indicates a quite different reactivity for dichloromethylene functions if incorporated into 5- or 7-membered rings. Interestingly, all investigated (co)polymers show an intrinsic microporosity in the solid-state (forming so-called Conjugated Polymers of Intrinsic Microporosity C-PIMs) and have S_{BET} values of up to 760 m^2 g^{-1} for homopolymer **P77**. This value is one of the highest reported values to date for C-PIMs.

Introduction

The reductive dehalogenation polycondensation of fully aromatic "bisgeminal tetrachlorides" as reactive diketone derivatives for the synthesis of π-conjugated poly(arylenevinylene)s was pioneered by Hans-Heinrich Hörhold and co-workers in the 1970s[1,2] Initially, chromium(II)acetate ($Cr_2(OAc)_4$) was used as an efficient dehalogenating reagent in polar solvents such as THF or DMF, or in solvent mixtures containing THF or DMF.[1,2] Later, we were successful in generating structurally related, but more highly condensed poly(indenofluorene) **PIF/P55** and poly(diindenonaphthalene) **PDIN** (Scheme 1), whereby the penta- or hexacyclic building blocks are connected *via* exocyclic double bonds that are made through a reductive polyolefination process; this produces polymers with on-chain bifluorenylidene structural motifs (Scheme 1, the bifluorenylidene unit is labeled in red).[3–5] Later, we tested the application of other dehalogenation agents, such as $Co_2(CO)_8$ [6,7] or $Ni(COD)_2$ [8] in chlorobenzene as the suitable non-polar solvent. The products poly(indenofluorene) **P55** and poly(diindenonaphthalene) **PDIN** are low bandgap polyhydrocarbons with

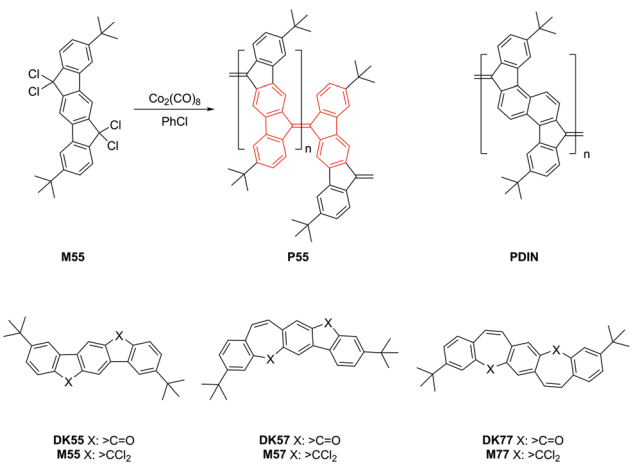

Scheme 1 Top: Chemical structures of **P55** and **PDIN**, as well as the principle of the reductive dehalogenation polycondensation, examplified for the synthesis of **P55**. Bottom: Chemical structures of monomers **M55**, **M57** and **M77**, the tetrabenzopentafulvalene (**TBPF**, bifluorenylidene) motif is highlighted in red.

[a]*Macromolecular Chemistry, University of Wuppertal, Gaussstrasse 20, 42119 Wuppertal, Germany. E-mail: scherf@uni-wuppertal.de*
[b]*Materials Innovation Factory, University of Liverpool, 51 Oxford Street, Liverpool, L7 3NY, UK*

†Electronic supplementary information (ESI) available: Monomer and polymer synthetic procedures for new compounds, NMR data, optical spectra, PXRD patterns for polymers, gas sorption data, TGA data, SEM images. See DOI: 10.1039/c9py00869a

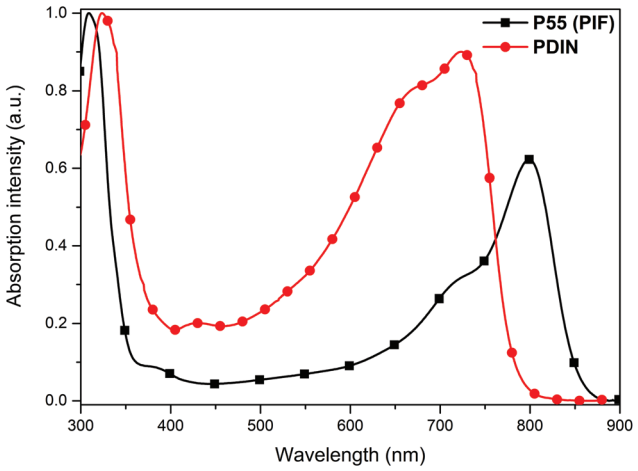

Fig. 1 UV-Vis spectra of **P55** and **PDIN** in chloroform solutions, λ_{max} **P55**: 799 nm (M_n = 17 000 g mol^{-1}), λ_{max} **PDIN**: 724 nm (M_n = 30 000 g mol^{-1}), $\Delta\lambda$ = 75 nm (0.16 eV); for **P55** a LUMO energy level of *ca.* 3.95 eV and a HOMO energy level of *ca.* 5.25 eV were estimated, from ref. 3 and 4.

long wavelength absorption features ranging into the near infrared (NIR) region. The low bandgap character (Fig. 1), with significantly red-shifted long wavelength absorption bands, was assigned to the contribution of quinoidal resonance states to the electronic ground state. We suggested this was mainly driven by the presence of twisted exocyclic double bonds as result of the crowded steric situation around these double bonds.[3,4]

Results and discussion

In this work, we develop related pentacyclic tetrachloro-monomers that contain 7-membered (cycloheptatriene) instead of the initially used 5-membered (cyclopentadiene) connector rings by introducing one or two additional vinylene groups into the monomers (Scheme 1). With this set of three monomers (3,9-di-*tert*-butyl-6,6,12,12-tetrachloro-6,12-dihydroindeno[1,2-*b*]fluorene **M55**: the already tested indenofluorene-based monomer for **P55** synthesis, 2,8-di-*tert*-butyl-6,6,14,14-tetrachloro-6,14-dihydrobenzo[4,5]cyclohepta[1,2-*b*]fluorene **M57**, and 3,11-di-*tert*-butyl-5,5′,13,13′-tetrachlor-dibenzo[*d*,*d*′]benzo[1,2-*a*:4,5-*a*′]di[7]annulene **M77**) we have carried out a series of reductive dehalogenation polycondensation reactions, including that of the known homopolymer **P55** – the already well-known poly(indenofluorene) **PIF**, and of the new homopolymers **P57** (resulting from polycondensation of the AB-type monomer **M57**) and **P77** (resulting from polycondensation of monomer **M77**) as well as a copolymer **P55/77** resulting from polycondensation of a 1 : 1 molar mixture of monomers **M55** and **M77** (in a AA/BB copolymerization scheme).

First, we studied the homopolycondensation of monomer **M77** yielding **P77**: as a corresponding dimeric model compound – tetrabenzoheptafulvalene (**TBHF**) (Scheme 2, red labeled part) – it is well known that a strongly folded, *anti*- or *syn*-type isomeric arrangement of the two non-planar, boat-shaped dibenzannelated 7-membered cycloheptatriene rings is adopted with nearly no electronic (conjugative) interaction across the exocyclic double bond. This was first derived from a NMR-spectroscopic analysis, and later complemented by single crystal structure analysis of both isomers.[9–12] This arrangement is in strong contrast to the electronic properties of the tetrabenzopentafulvalene (bifluorenylidene, **TBPF**) system with its *ca.* 42° twisted exocyclic double bond that connects two, almost planar fluorenylidene units.[13,14] Next, we tested the polycondensation of the "mixed" monomer **M57** that contains one 5- and 7-membered ring each[15] and, for comparison, of a 1 : 1 **M55**/**M77** monomer mixture. Since we expect a quite different reactivity of both geminal >CCl_2-functions in the reductive polyolefination when incorporated into 5- or 7-membered rings, we investigated the incorporation pattern of the monomeric subunits into the resulting fulvalene linkages in more detail. In particular, we compared chemical structure and optical/electronic properties of homopolymer **P57** and copolymer **P55/77**.

Monomer and polymer synthesis

As mentioned above, reductive polycondensation of the tetrachloro monomers **M77** and **M57** gives homopolymers **P77** and **P57**, respectively. The non-alkylated analogues of the diketone model compounds **DK77** and **DK57** were already described in the literature.[16,17] Instead of following the published route for non-alkylated **DK77**, we adapted a more recent route published by Yang *et al.*[15] for **DK57**, starting for both monomers from 2,5-dibromoterephthalic acid, which is a frequently used starting material for ladder-type polyarylenes made by us previously.[18,19]

For the synthesis of **M57** and **M77**, we used an elegant procedure by Ciganek *et al.* involving a one-pot dehydrogenation/chlorination of the corresponding, single- or double-ethane-bridged diketones **5**.[20] In contrast to the corresponding five-ring or acyclic tetrachloro derivatives,[3,4,6,7] the bisgeminal tetrachlorides containing seven-membered rings are much more air sensitive: simple recrystallisation from *n*-hexane or toluene under air yielded the unsaturated diketone derivatives, indicated by the occurrence of keto carbon resonances at around 190 ppm in the $^{13}C\{^1H\}$ NMR spectra. Therefore, after removal of excess $POCl_3$/toluene and PCl_5 by vacuum distillation and sublimation, the air sensitive compounds **M57** and **M77** were directly used in the subsequent polycondensation reactions with dicobalt octacarbonyl in chlorobenzene without further purification to give **P57** and **P77**, respectively. **P55/77** was obtained by chlorination of **5a** and **5b** to give **M55** and **M77**, respectively, followed by subsequent polycondensation of the 1 : 1 monomer mixture.

Homopolymer P77

Polymer **P77** was obtained as yellow powder after work-up and solvent fractionation using Soxhlet extraction, with molecular weight (MW) averages M_n of 9500 (DP: *ca.* 22) for the minority ethyl acetate fraction (16%), and M_n of 4550 (DP: *ca.* 10) for the main, lower molecular weight acetone fraction (81%) thus confirming the successful polycondensation up to the polymer

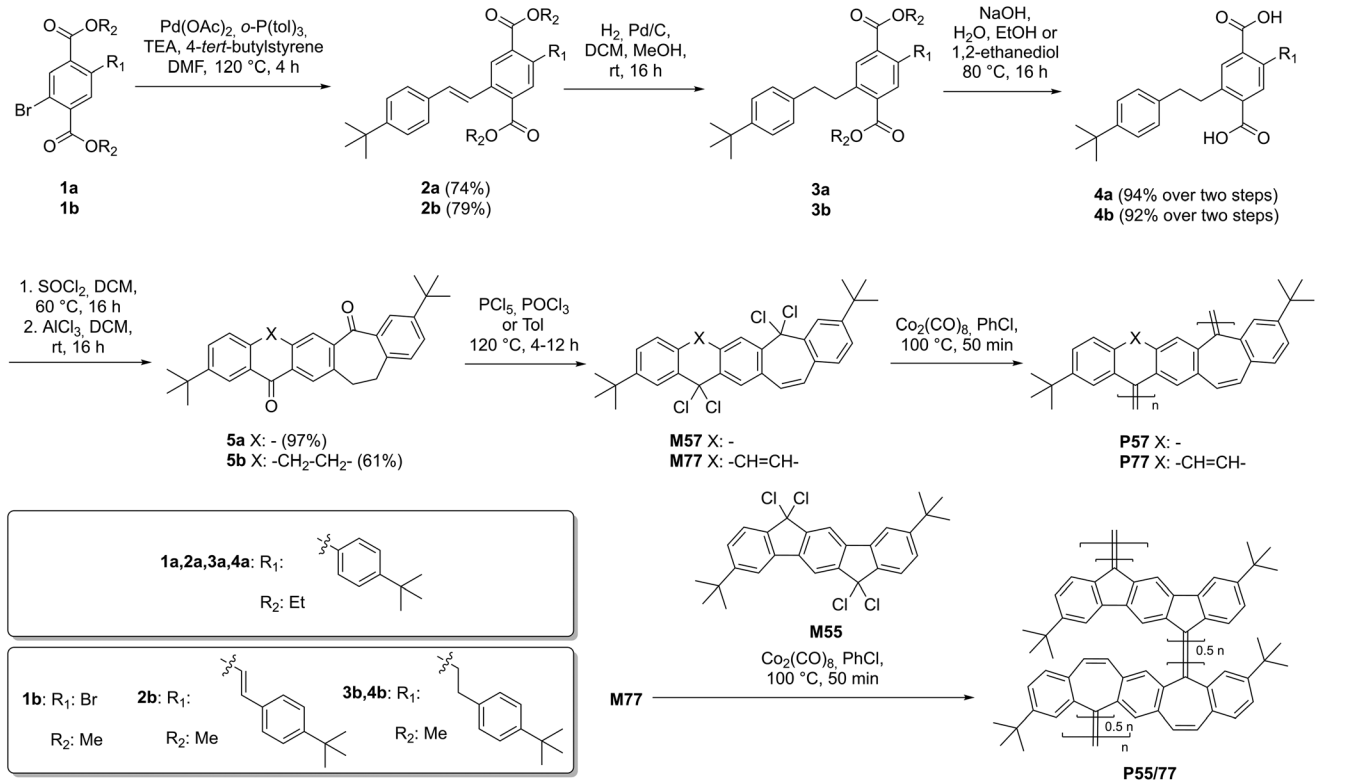

Scheme 2 Syntheses scheme for monomers **M57** and **M77** as well as homopolymers **P77** and **P57**, and copolymer **P55/77**.

limit despite the highly sterically demanding environment around the coupling positions. In the $^{13}C\{^1H\}$ NMR spectrum of **P77**, the two aliphatic carbon signals of the *tert*-butyl side groups are doubled, probably indicating the presence of both *cis*- (*Z*-) and *trans*- (*E*-) isomeric arrangements of the pentacyclic repeating units with respect to the exocyclic double bonds (Scheme 3 depicts the *trans* configuration). The aromatic ^{13}C NMR signals of **P77** are distinctly broadened as consequence of the polymer formation (for ^1H and $^{13}C\{^1H\}$ NMR spectra see Fig. S13 in the ESI†).

Fig. 2 shows the optical spectra of **P77** (higher MW ethyl acetate fraction) and the corresponding diketone precursor **DK77** in diluted chloroform solution. The absorption range is restricted to the UV region due to the strongly folded structure of the polymer. The diketone **DK77** shows a low intensity long wavelength n–π* transition (as shoulder at *ca.* 430 nm) and a higher intensity π–π* transition peaking at *ca.* 361 nm. In the polymer, the π–π* transition-related band is blue-shifted to 331 nm by $\Delta\lambda$ = 30 nm, thus reflecting the presence of loca-

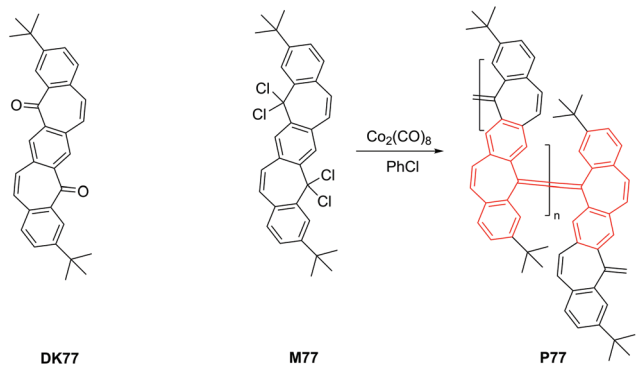

Scheme 3 Synthesis of **P77** by reductive polycondensation of the tetrachloro monomer **M77**, the tetrabenzoheptafulvalene (**TBHF**) moiety is labeled in red; on the left side, the chemical structure of the corresponding diketone precursor **DK77** is also shown.

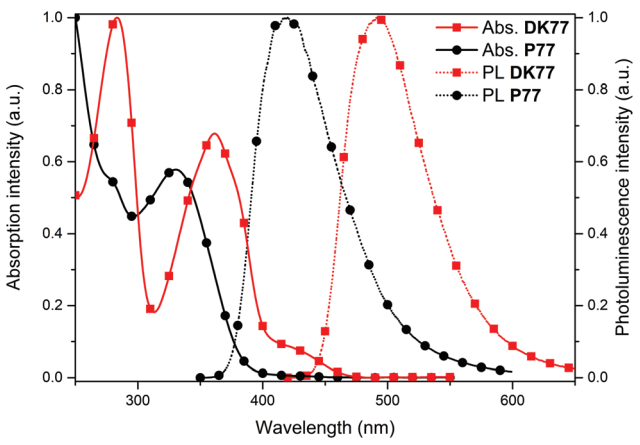

Fig. 2 Absorption and photoluminescence spectra of **P77** and the corresponding diketone precursor **DK77** (solvent: chloroform, excitation wavelength λ_{exc}: 310 nm for **P77**, and 330 nm for **DK77**.

lised, isolated chromophores with the electronic interaction restricted to one *cis*-distyrylbenzene unit, and without noticeable conjugation across the folded exocyclic double bond. The photoluminescence spectra of precursor diketone **DK77** and polymer **P77** display emission maxima (0-0 transitions) at λ_{max} (PL) of 492 nm for the diketone and a hypsochromically shifted deep blue PL peaking at 419 nm for the polymer **P77** ($\Delta\lambda$ = 73 nm, photoluminescence quantum yield PLQY of **P77** in chloroform solution: 2.54%). The absorption spectrum of **P77** as a thin-film (see Fig. S24 in the ESI†) only shows a low intensity shoulder in the region of the long wavelength absorption band of the chloroform solution (*ca.* 340 nm), without any longer wavelength absorption features.

Homopolymer P57 and Copolymer P55/77

The synthesis of a non-alkylated analogue of **M57** was already described in the literature.[13] The alkylated analogue was generated as depicted in Scheme 2, the finally prepared bisgeminal tetrachloride **M57** was obtained by reaction of the diketone precursor with phosphorous pentachloride. Due to its air sensitivity the monomer was directly used in a reductive olefination reaction with dicobalt octacarbonyl. After work-up and solvent fractionation, **P57** was obtained as red powder with M_n: 10 400 (DP: *ca.* 26) for the ethyl acetate fraction (33%), while the lower molecular weight acetone fraction (51%) showed a molecular weight M_n of 3600 (DP: *ca.* 9). In contrast to **P77**, in the $^{13}C\{^1H\}$ NMR spectrum of **P57**, the aliphatic signals are not clearly doubled which may be a result of the asymmetry of the repeat unit (for the related ^1H and $^{13}C\{^1H\}$ NMR spectrum of the diketone **DK57** see Fig. S12 in the ESI†).

P55/77 was obtained in a random copolymerisation of monomers **M55** and **M77**. Hereby, equimolar amounts of both diketone precursors were chlorinated. After removal of solvents/$POCl_3$ and sublimation of excess PCl_5, both products were dissolved in chlorobenzene and reacted in a reductive copolycondensation with dicobalt octacarbonyl. After work-up and solvent fractionation, the product **P55/77** was obtained as a deep blue powder, with a M_n of 5500 (DP: *ca.* 14) for the ethyl acetate fraction (13%), while the lower molecular weight acetone fraction (21%) has a M_n of 2900 (DP: *ca.* 7).

The very similar positions of the absorption maxima of **P57** at 485 nm and the isolated **TBPF** chromophore (λ_{max}: 460 nm, see Fig. 3)[21] indicates the dominating presence of alternating twisted **TBPF** and folded **TBHF** motifs in **P57** as consequence of a very different reactivity of the two different dichloromethylene functions of **M57** during the reductive polycondensation, with the higher reactivity most probably for the sterically less stressed –CCl_2– units incorporated into 5-membered rings. Hereby, the **TBHF** building blocks formed in the second condensation step act as efficient conjugation barriers and lead to the presence of isolated **TBPF** chromophores within the polymer main chain that is composed in an alternating order of **TBHF** and **TBPF** units. Moreover, the distinctly red-shifted absorption band of **P55/77** peaking at 705 nm, if compared to **P57** (486 nm), indicates the presence of more extended, π-conjugated oligoindenofluorene segments (for a

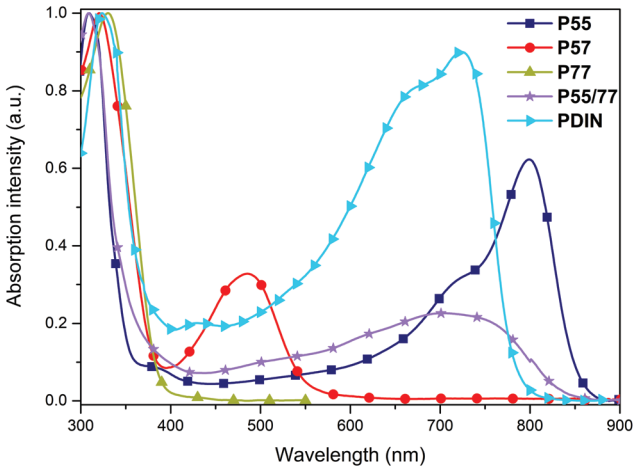

Fig. 3 UV-Vis spectra of **P55**, **P57**, **P77**, **P55/77** and **PDIN** in chloroform solution.

study of the absorption properties of **M55**-derived oligomers see ref. 22) as consequence of the preferred coupling of the sterically less demanding dichloromethylene functions of **M55**, thus resulting in a tendency for (multi)block copolymer formation. Similar results have been described for the Yamamoto-type polycondensation of two different dibromoarylene/dibromoheteroarylene monomers.[23]

Gas sorption

Linear and soluble polymers of intrinsic microporosity (so-called PIMs) have been known since the pioneering work of Budd, McKeown and co-workers.[25,26] Several folding motifs, including on-chain spirobifluorene[27,28]/spirobiindane,[29] binaphthyl,[30] triptycene[31] or norbornyl bis(benzocyclobutene)[32] units, have been introduced to give a shape-persistent folding of rigid-rod type polycyclic segments of linear polymer chains that pack into bulk materials with a persistent free volume.[33] Also several conjugated polymers (CPs) with bulky main chain substituents, including poly(trimethylsilylacetylene)s[34] or poly(diphenylacetylene)s[35] and CPs containing 1,3-phenylene units[36–39] show a permanent microporosity with S_{BET} surface areas up to 730 $m^2\ g^{-1}$ (so-called conjugated PIMs—C-PIMs). Based on these concepts we have tested if the incorporation of strongly folded tetrabenzoheptafulvalene (**TBHF**) or twisted bifluorenylidene motifs into the linear, polycyclic homopolymers **P55**, **PDIN**, **P77** and **P57** as well as the copolymer **P55/77** also induces a permanent microporosity. For the already known **P55** and **PDIN**, we expected the materials to be microporous due to the twisted bifluorenylidene motifs, which is similar to the orthogonal spirobisindane motif in PIM-1.[24]

The microporosity properties of the polymers **P55**, **PDIN**, **P57**, **P77** and **P55/77** were studied by nitrogen gas adsorption/desorption measurements at 77 K. All polymers showed typical type-I isotherms with a significant amount of nitrogen adsorption at low pressure, indicating presence of micropores, a slowly increasing gas adsorption in the mid pressure range,

Table 1 Molecular weights and DPs of the high MW fractions, absorption maxima and gas sorption data of the polymers and copolymers investigated

Polymer	M_n (kDa)	M_w (kDa)	M_w/M_n	DP	λ_{max} (nm)	S_{BET} ($m^2\ g^{-1}$)	V_{total} ($cm^3\ g^{-1}$)	V_{micro} ($cm^3\ g^{-1}$)	H_2 uptake (77 K)[a] (mmol g^{-1})	CO_2 uptake (273 K)[a] (mmol g^{-1})
P77	9.5	20.2	2.1	23	331	757[b]	0.58	0.22	5.1	1.8
P57	10.4	14.4	1.4	26	485, 321	609	0.39	0.17	4.3	1.6
P55/77	5.5	7.4	1.4	14	705, 309	543	0.41	0.15	3.6	1.2
P55 (PIF)	17.0	40.0	2.4	47	799, 309	687[c] (738[d]; 333[e])	0.51	0.18	4.6	1.6
PDIN	25.0	57.0	2.3	61	724, 324	691[f]	0.68	0.16	4.1	1.4

[a] Uptake at 1 bar. [b] Powder sample with a M_n: 13.2 kDa, M_w: 20.7 kDa. [c] Powder sample with a M_n: 7.2 kDa; M_w: 13.9 kDa. [d] After $scCO_2$ washing of a powder sample with M_n: 7.2 kDa; M_w: 13.9 kDa. [e] After drop-casting the sample from chloroform solution. [f] Powder sample with M_n: 5.3 kDa; M_w: 11.0 kDa.

followed by increased adsorption at higher relative pressure ($P/P_0 > 0.9$) especially for **PDIN**, probably caused by multilayer formation in meso- or macropores (see Fig. S17 in the ESI†). Differential pore size distributions obtained by application of hybrid density functional theory confirmed the mostly microporous nature of the polymers, with the maximum values in the range of 1–2 nm (see Fig. S20 in the ESI†). We observed a pronounced hysteresis between adsorption and desorption curves, which may either be attributed to pore network effects and various forms of pore blocking with capillary condensation or to swelling effects that were also observed for other PIMs and flexible, amorphous networks.[24,40–43] PXRD patterns confirmed the amorphous nature for all polymers discussed here (see Fig. S22 in the ESI†).

The estimated surface areas for the polymers ranged from 543 $m^2\ g^{-1}$ for **P55/77** to 757 $m^2\ g^{-1}$ for **P77** (see Table 1), comparing well with the currently highest reported values for C-PIMs (see Table S1 in the ESI† for a comparative listing of literature values). Interestingly, a drop-casted thin film of **P55** maintained its microporosity to nitrogen and showed a S_{BET} surface area of 333 $m^2\ g^{-1}$, thus demonstrating strong potential for future practical applications. Considering the strong influence of processing conditions on the apparent surface area of soluble porous polymers, we tested additionally washing a freshly precipitated powder sample with supercritical carbon dioxide ($scCO_2$), which proved to strongly affect the S_{BET} surface area in the past.[44] The S_{BET} surface area only slightly increased when a powder sample of **P55** was additionally purified by supercritical carbon dioxide $scCO_2$ washing (738 *vs.* 687 $m^2\ g^{-1}$) thus confirming a reliable sample preparation protocol. Sorption isotherms as well as SEM images of powder and film indicated very different morphologies with a substantial loss of meso- and macroporosity for the film, probably causing the decreased overall S_{BET} surface area (see Fig. S23 in the ESI†).

To explore the potential for gas storage- or separation, we conducted sorption measurements using carbon dioxide (at 273 K) and hydrogen (at 77 K) (see Fig. S19 in the ESI†). Interestingly, **P57** showed a higher uptake for carbon dioxide and hydrogen than **PDIN**. A possible explanation might be that micropores of **P57** may be inaccessible for N_2, but accessible to CO_2 and H_2. The highest uptakes (see Table 1) of 1.8 mmol g^{-1} CO_2 and 5.1 mmol g^{-1} H_2 at *ca.* 1 bar for **P77**, comparing well with other highly porous C-PIMs.[37]

Conclusions

In summary, we present the synthesis of three novel homo- and copolymers **P77**, **P57** and **P55/77**, where pentacyclic building blocks are linked together by exocyclic double bonds, in addition to the already known **P55** and **PDIN**. The (co)polymers are made by reductive dehalogenation polycondensation of pentacyclic, bisgeminal tetrachlorides with dicobalt octacarbonyl, a protocol that was established by our group. All monomers contain reactive dichloromethylene functions that are incorporated into 5- or 7-membered rings. The results presented here indicate an interrupted conjugation along exocyclic double bonds for the tetrabenzoheptafulvalene (**TBHF**) connector, while tetrabenzopentafulvalene (**TBPF**) connectors allow for a main chain π-electron delocalization. This leads to quite different optical (absorption) spectra of the polymers, for the polymer **P77** containing exclusively **TBHF** connections the absorption range is restricted to the UV area. By introducing **TBPF** motifs into the polymer backbone, the long wavelength absorption band is gradually red-shifted in parallel with the length of the present conjugated segments. These results also indicate a higher reactivity of the bisgeminal dichlorides that are incorporated into 5-membered rings, supported by the obvious formation of multiblock copolymers for **M55/M77** monomer mixtures and by the formation of alternating **TBHF** and **TBPF** connections during coupling of **M57** into **P57**.

All (co)polymers are microporous and constitute new examples of the relatively uncommon sub-class of materials known as 'Conjugated Polymers of Intrinsic Microporosity' (C-PIMs). BET surface areas are as high as 757 $m^2\ g^{-1}$. All (co)polymers showed S_{BET} surface areas in a narrow range between 500 to 800 $m^2\ g^{-1}$. These results impressively demonstrate that both non-planar, twisted tetrabenzopentafulvalene (**TBPF**, bifluorenylidene) as well as folded tetrabenzoheptafulvalene (**TBHF**) motifs both induce a significant intrinsic microporosity of the linear C-PIMs in the solid state, thus representing very promising building blocks in the development of functional C-PIMs.

Conflicts of interest

There are no conflicts to declare.

Acknowledgements

The authors would like to thank Sylwia Adamczyk and Dr. Ammar H. Alahmed for help with gas sorption, Anke Helfer for the GPC, and Andreas Siebert for NMR measurements. We thank the Engineering and Physical Sciences Research Council (EPSRC) for financial support under Grant EP/N004884/1.

Notes and references

1 H.-H. Hörhold, J. Gottschaldt and J. Opfermann, *J. Prakt. Chem.*, 1977, **319**, 611.
2 H.-H. Hörhold and D. Raabe, *Acta Polym.*, 1979, **30**, 86.
3 H. Reisch, U. Wiesler, U. Scherf and N. Tuytuylkov, *Macromolecules*, 1996, **29**, 8204.
4 E. Preis and U. Scherf, *Macromol. Rapid Commun.*, 2006, **27**, 1105.
5 E. J. Meijer, D. M. de Leeuw, S. Setayesh, E. van Veenendaal, B.-H. Huisman, P. W. M. Blom, J. C. Hummelen, U. Scherf and T. M. Klapwijk, *Nat. Mater.*, 2003, **2**, 678.
6 E. Preis, W. Dong, G. Brunklaus and U. Scherf, *J. Mater. Chem. C*, 2015, **3**, 1582.
7 S. Baysec, E. Preis and U. Scherf, *Macromol. Rapid. Commun.*, 2016, **37**, 1802.
8 H. Reisch, *Oligo- und Poly(indenofluorene) – neue Materialien mit einer kleinen Bandlücke*, PhD Thesis, University of Mainz, Germany, 2000.
9 W. Treibs and H.-J. Klinkhammer, *Chem. Ber.*, 1951, **84**, 671.
10 A. Schönberg, U. Sodke and K. Praefcke, *Chem. Ber.*, 1969, **102**, 1453.
11 K. S. Dichmann, S. C. Nyburg, F. H. Pickard and J. A. Potworowski, *Acta Crystallogr., Sect. B: Struct. Crystallogr. Cryst. Chem.*, 1974, **30**, 27.
12 J. Luo, K. Song, F. I. Gu and Q. Miao, *Chem. Sci.*, 2011, **2**, 2029.
13 A. Takai, D. J. Frea, T. Suzuki, M. Sugimoto, J. Labuta, R. Haruki, R. Kumai, S.-I. Adachi, H. Sakai, T. Hasobe, Y. Matsushita and M. Takeuchi, *Org. Chem. Front.*, 2017, **4**, 650.
14 P. U. Biedermann, J. J. Stezowski and I. Agranat, *Eur. J. Org. Chem.*, 2001, 15.
15 X. Yang, X. Shi, N. Aratani, T. P. Goncalves, K.-W. Huang, H. Yamada, C. Chi and Q. Miao, *Chem. Sci.*, 2016, **7**, 6176.
16 I. Agranat and D. Avnir, *J. Chem. Soc., Perkin Trans. 1*, 1974, 1155.
17 X. Yang, D. Liu and Q. Miao, *Angew. Chem., Int. Ed.*, 2014, **53**, 6786.
18 K.-J. Kass, M. Forster and U. Scherf, *Angew. Chem., Int. Ed.*, 2016, **55**, 7816.
19 M.-C. Ockfen, M. Forster and U. Scherf, *Macromol. Rapid Commun.*, 2018, 1800569.
20 E. Ciganek, R. T. Uyeda, M. Cohen and D. H. Smith, *J. Med. Chem.*, 1981, **24**, 336.
21 F. Straus, R. Kühnel and R. Hänsel, *Ber. Dtsch. Chem. Ges. A/B*, 1933, **66**, 1847.
22 H. Reisch and U. Scherf, *Synth. Met.*, 1999, **101**, 128.
23 U. Asawapirom and U. Scherf, *Macromol. Rapid Commun.*, 2001, **22**, 746.
24 P. M. Budd, B. S. Ghanem, S. Makhseed, N. B. McKeown, K. J. Msayib and C. E. Tattershall, *Chem. Commun.*, 2004, **2**, 230.
25 P. M. Budd, E. S. Elabas, B. S. Ghanem, S. Makhseed, N. B. McKeown, K. J. Msayib, C. E. Tattershall and D. Wang, *Adv. Mater.*, 2004, **16**, 456.
26 P. M. Budd, K. J. Msayib, C. E. Tattershall, B. S. Ghanem, K. J. Reynolds, N. B. McKeown and D. Fritsch, *J. Membr. Sci.*, 2005, **251**, 263.
27 J. Weber, Q. Su, M. Antonietti and A. Thomas, *Macromol. Rapid Commun.*, 2007, **28**, 1871.
28 D. Becker, N. Konnertz, M. Böhning, J. Schmidt and A. Thomas, *Chem. Mater.*, 2016, **28**, 8523.
29 P. M. Budd, N. B. McKeown and D. Fritsch, *Macromol. Symp.*, 2006, **245**, 403.
30 N. Ritter, M. Antonietti, A. Thomas, I. Senkovska, S. Kaskel and J. Weber, *Macromolecules*, 2009, **42**, 8017.
31 B. S. Ghanem, M. Hashem, K. D. M. Harris, K. J. Msayib, M. Xu, P. M. Budd, N. Chaukura, D. Book, S. Tedds, A. Walton and N. B. McKeown, *Macromolecules*, 2010, **43**, 5287.
32 H. W. H. Lai, Y. Chin and Y. Xia, *ACS Macro Lett.*, 2017, **6**, 1357.
33 P. M. Budd and N. B. McKeown, *Chem. Soc. Rev.*, 2006, **35**, 675.
34 T. Masuda, E. Isobe, T. Higashimura and K. Takada, *J. Am. Chem. Soc.*, 1983, **105**, 7473.
35 W.-E. Lee, D.-C. Han, D.-H. Han, H.-J. Choi, T. Sakaguchi, C.-L. Lee and G. Kwak, *Macromol. Rapid Commun.*, 2011, **32**, 1047.
36 G. Cheng, T. Hasell, A. Trewin, D. J. Adams and A. I. Cooper, *Angew. Chem., Int. Ed.*, 2012, **124**, 12899.
37 G. Cheng, B. Bonillo, R. S. Sprick, D. J. Adams, T. Hasell and A. I. Cooper, *Adv. Funct. Mater.*, 2014, **24**, 5219.
38 R. S. Sprick, J.-X. Jiang, B. Bonillo, S. Ren, T. Ratvijitvech, P. Guiglion, M. A. Zwijnenburg, D. J. Adams and A. I. Cooper, *J. Am. Chem. Soc.*, 2015, **137**, 3265.
39 R. S. Sprick, Y. Bai, A. A. Y. Guilbert, M. Zbiri, C. M. Aitchison, L. Wilbraham, Y. Yan, D. J. Woods, M. A. Zwijnenburg and A. I. Cooper, *Chem. Mater.*, 2019, **31**, 305.
40 S. Qiao, Z. Du and R. Yang, *J. Mater. Chem. A*, 2014, **2**, 1877.
41 J. Weber and A. Thomas, *J. Am. Chem. Soc.*, 2008, **130**, 6334.
42 N. B. McKeown, S. Hanif, K. Msayib, C. E. Tattershall and P. M. Budd, *Chem. Commun.*, 2002, **23**, 2782.
43 J. Jeromenok and J. Weber, *Langmuir*, 2013, **29**, 12982.
44 E. Preis, C. Widling, U. Scherf, S. Patil, G. Brunklaus, J. Schmidt and A. Thomas, *Polym. Chem.*, 2011, **2**, 2186.